NUMERICAL TECHNIQUES FOR SCATTERING FROM SUBMERGED OBJECTS

Michael F. Werby and Gerald J. Tango
National Space Technology Laboratories
NSTL Station, Mississippi 39529-5004

G.C. Gaunaurd
Naval Surface Weapons Center
Silver Spring, Maryland 20910

Scattering from submerged objects consisting of separable boundaries, such as spheres and infinite cylinders, is amenable to closed-form solution by normal mode theory. Results from extensive investigations of these objects has been extremely fruitful in understanding resonance phenomena, background contributions in the absence of resonances, and geometrical effects that give rise to diffraction phenomena. However, when one wishes to examine arbitrary shapes, it is necessary to resort either to approximate theories (valid under limiting assumptions) or numerical methods that adequately treat the problem in question. It has, in fact, proven very difficult to describe scattering from general objects without resorting to frequency-limiting approximations. In this Forum, we describe a numerical procedure, namely, the "extended boundary condition" (EBC) method, together with its applications for treating a variety of problems. The method was established by Waterman[1] for electromagnetic scattering in 1965, and was extended to acoustical scattering by him in 1969[2]. It is sometimes referred to as the "null-field" method in electromagnetism, the "field equivalent principle," or more generally as the T-matrix method. This last nomenclature is unfortunate, since any of a variety of methods can lead to a transition matrix relating the scattered to the incident field, while the EBC or null-field terminology more properly reflects the fact that one is employing a boundary integral technique.

Some of the salutary features of this approach are that (1) the method yields unique solutions to the exterior problem; (2) the transition matrix is independent of the incident field; (3) the method is not frequency-limiting, though it is more efficient for intermediate frequencies; (4) the method can work for a large variety of shapes.

To represent the final results in terms of matrices, one expands all appropriate physical quantities in terms of partial wave basis states. This includes expansions for the incident and scattered fields and the surface quantities (i.e., surface displacement, surface traction, etc.). The method then utilizes the Huygen-Poincaré integral representation for both the exterior and interior solutions, leading to the required matrix equations. One thus deals with matrix equations, the complexity of which depends on the nature of the problem. We show, however, that in general a transition matrix T can be obtained relating the incident field A with the scattered field f having the form $T = PQ^{-1}$, where $f = TA$. The structure of Q can be quite complicated and can itself be composed of other matrix inversions such as arise from layered objects. We focus on recent improvements in this method appropriate for a variety of physical problems, and on their implementation. We outline results from scattering simulations for very elongated submerged objects and resonance scattering from elastic solids and shells. Significant structural improvements such as the coupled higher-order method[3], and the unitary method[4], which lead to more tractable forms of the transition matrix enabling one to avoid matrix inversions and other numerical problems. The final improvement concerns eigenfunction expansions of surface terms, arising from solution of the interior problem, obtained via a preconditioning technique. This effectively reduces the problem to that of obtaining eigenvalues of a Hermitian operator.

This formalism is reviewed for scattering from targets that are rigid, sound-soft, acoustic, elastic solids, elastic shells, and elastic layered objects. We present two sets of the more interesting results. The first concerns scattering from elongated objects, and the second to thin elastic spheroids.

Figure 1 illustrates scattering from a spheroid with aspect ratio 30 for a KL/2 value of 30. Here K is the incident wavenumber and L the object length. We show the case of scattering along the axis of symmetry and 30° and 60° relative to the axis of symmetry and broadside. Elongation effects at 30° and 60° are particularly noticeable where the reflected wave occurs at the same angle as the incident wave relative to the symmetry axis, similar to the plane scattering case. At 0° and 90° the flux is allowed to proceed mainly in the forward direction, with broadside scattering creating the greatest disturbance.

Figure 2a shows resonance phenomena from backscattering from a very thin aluminum spheroid, plotted against KL/2. Scattering here occurs along the axis of symmetry for a spheroid of aspect ratio 3-to-1. Because of the thin nature of the object, its scattering response is like that of a sound-soft object in the absence of resonance. This is verified by subtracting the sound-soft background from the exact elastic calculation, leaving only the resonance response (Figure 2b). Figure 2c is a plot of relative phase for the elastic and sound-soft calculations. Note that the phase is almost zero except at a resonance, where it undergoes a rapid phase-change of 180°, typical of this type of resonance.

REFERENCES

1. P. C. Waterman, "Matrix formulation of electromagnetic scattering," *Proc. IEEE*, 53, 805 (1965).
2. P. C. Waterman, "New foundations of acoustic scattering," *J. Acoust. Soc. Am.*, 45, 1417 (1969).
3. M. F. Werby, "A coupled high-order T-matrix," *J. Acoust. Soc. Am.* (to appear) (1985).
4. M. F. Werby and L. H. Green, "An extended unitary approach-acoustical scattering from elastic shells immersed in a fluid," *J. Acoust. Soc. Am.*, 74, 625 (1983).

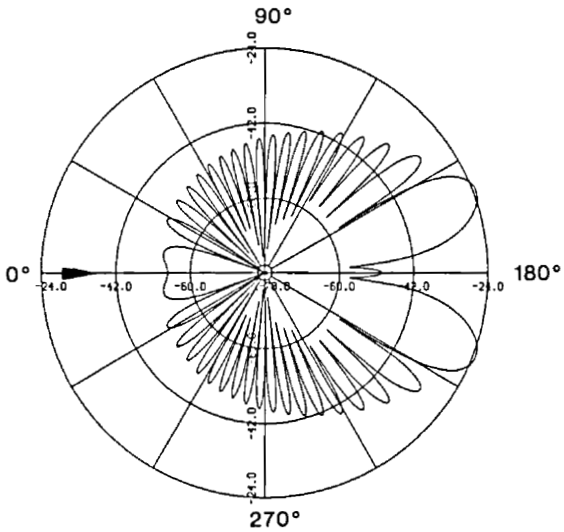

Figure 1a. Scattering along axis of symmetry of spheroid.

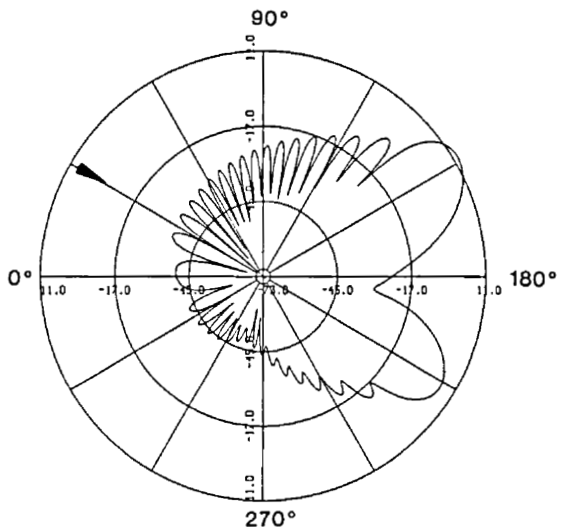

Figure 1b. Scattering at 30° relative to the axis of symmetry of spheroid.

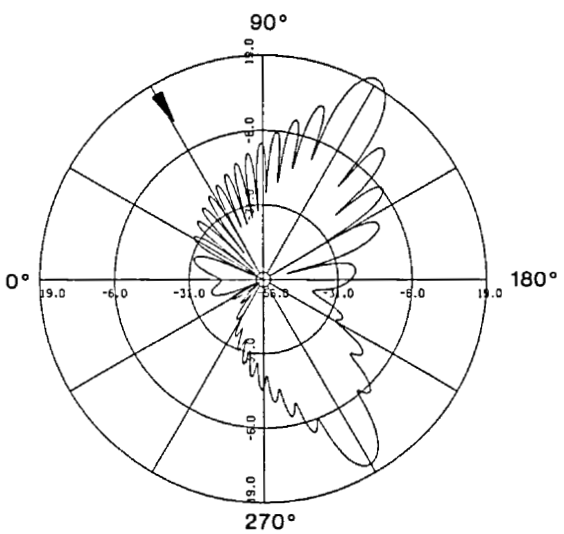

Figure 1c. Scattering at 60° relative to the axis of symmetry of spheroid.

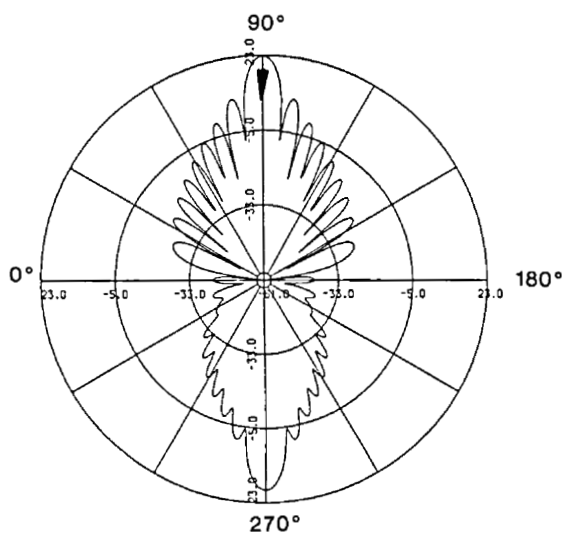

Figure 1d. Broadside scattering from a spheroid.

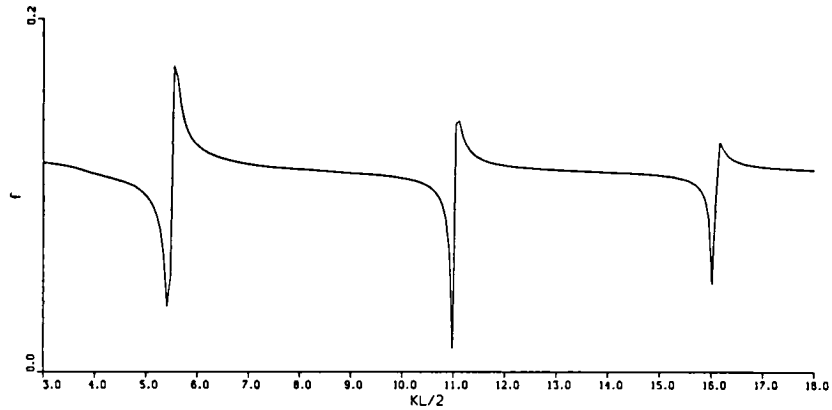

Figure 2a. Form function plot of elastic spheroid end-on incidence.

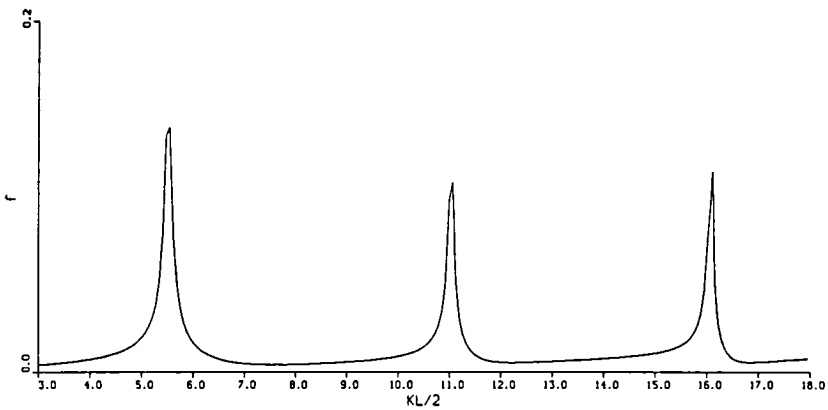

Figure 2b. Resonance response of elastic spheroid end-on incidence.

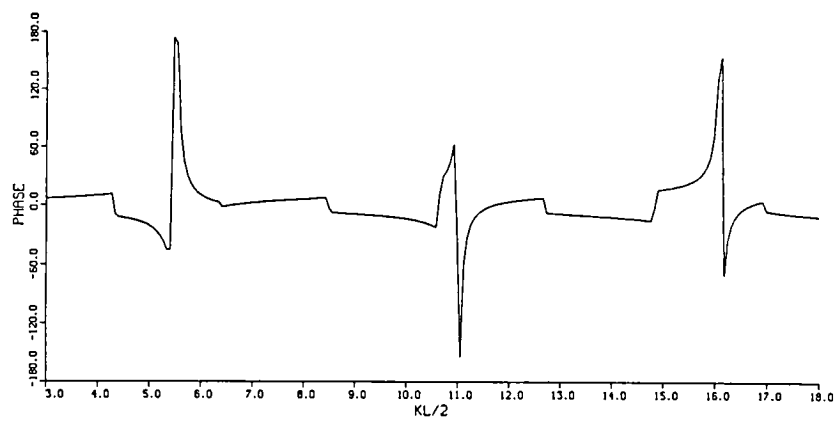

Figure 2c. Relative phase between elastic thin shell and sound-soft object.